

# Index Noise Comfort Inside a Vehicle for the Passengers from Tire/Road Interaction

Shawki Abdelhady Abouel-seoud, Mohamed Watany Mohamed Elsid, Nagwa Ahmed Abdel-halim, Eid Saber Mohamed, Ahmed Sultan Abdallah

Automotive Engineering Department, Faculty of Engineering, Helwan University, Cairo, Egypt

## Email address

s\_a\_seoud@hotmail.com (S. A. Abouel-seoud), watany@gmail.com (M. W. M. Elsid), nagwaibrahim2006@yahoo.co.uk (N. A. Abdel-halim), eng\_eid74@yahoo.com (E. S. Mohamed), engahmed\_sultan@yahoo.com (A. S. Abdallah)

## To cite this article

Shawki Abdelhady Abouel-seoud, Mohamed Watany Mohamed Elsid, Nagwa Ahmed Abdel-halim, Eid Saber Mohamed, Ahmed Sultan Abdallah. Index Noise Comfort Inside a Vehicle for the Passengers from Tire/Road Interaction. *International Journal of Public Health and Health Systems*. Vol. 2, No. 2, 2017, pp. 26-36.

**Received:** August 13, 2017; **Accepted:** November 23, 2017; **Published:** January 8, 2018

## Abstract

Discuss the potential criteria formats that can account for the interactive effects of noise on human discomfort response. The influence of driving speed, inflation pressure, tire type, road surface and preload are analysed. Practical measurements inside the vehicle of tire noise (a key used judged comfortability) and vibration amplitudes were conducted during coast down driving procedure. It is necessary to investigate a method of predicting road noise from multiple surfaces based on vehicle vibration measurement of a single surface to the design criteria aimed to improve the structural acoustic behaviour, to comply with the increasingly restrictive ergonomic standard. The approach used to estimate the vehicle acoustic comfort index depends on the measured and predicted sound pressure level (SPL) at the driver's head position, where SPL was calculated from the vehicle floor vibration under the driver's legs region based on the sample acoustic theory. This paper presents an overview of this approach development including the methodology with unloaded engine (neutral gear). The results indicate that the proposed approach was sensitive to changes in individual parameters. Hence it is very useful for making ride comfort design tradeoffs and as a tool for comparative assessment of ride comfort.

## Keywords

Acoustic Cavity, Interior Noise, Interior Vibration, Comfort Index, Vehicle Body Surface

## 1. Introduction

Noise comfort inside the vehicle is one of the main targets which may attract customers for purchasing a vehicle. Eventually, the ride discomfort comes from the vibration (magnitude, frequency, direction and, duration) exposition inside the cabin. The comfort of the driving is one of the parameters strongly influences the driving performances by bothering vision, and at the same time giving stress to the driver due to generated noise. The acoustic noise exposition depends on two main sources: engine and powertrain systems, and interaction between tyre and road surface. The sound quality assessment of a bi-fuel passenger car and perceived noise inside cabin tested over a chassis-dynamometer bench and analyzed at different vehicle operating conditions

assessing the influence on the driver's acoustic comfort [1, 2].

An approach has been carried out to find the amount of noise which influenced by the vibration due to interaction between tires and road surface. The sound quality analysis has been focused on the estimation of the noise changes through the generated sound quality depending on engine speeds, where the amount of sound quality followed the increase and decrease of the engine speeds. In addition, a technical method was provided to show the correlation between generated noise sound quality and the exposed vibration caused by the interaction between tires and road surface [3, 4].

Vehicle interior noise consists of a superposition of broadband contributions from powertrain, wind, and tire-road noise. Tire-road noise has become important referring to overall acoustic comfort, with pleasant low-noise engine

sounds. An interior noise recording during a coast-down (engine switched off) contains: a mixture of wind along with airborne and structure-borne tire-road noise shares. Appropriate algorithms and additional measurements are needed to separate the interior noise mixture into these components. Structure-borne excitation signals (airborne noise radiation) of all four tires are measured simultaneously to an artificial head recording inside the vehicle during a coast-down test from maximum speed to standstill [5].

The vehicle structural modes were analysed theoretically and sound radiation of a simply-supported rectangular panel. The 1<sup>st</sup> order vibration mode can be modelled as a point source radiator and simplified as a Single-Degree-Of-Freedom (SDOF) system with analysed the velocity transfer function characteristics. The relations among the panel's vibration, sound radiation and SDOF model were established. The mechanism of vehicle interior booming was provided, tested, identified, reduced and proposed the control method by tuning vehicle body panel's mass distribution that comes from the SDOF analysis. The analysis results have a good consistent with the test results and the simplified model provides a guideline for vehicle interior booming control [6-8].

The off-road and mid-size vehicles interior noise was measured while driving on three different asphalt road surfaces. The results indicated that the Vehicle Acoustic Comfort Factor (VACF) should be at lower level for a relatively high acoustical comfort and the kurtosis parameter value is greater in high roughness road surface at constant vehicle speed but is proportional to vehicle speed for every kind of road surface and it has inverse effect on VACF value. VACF is lesser for road surface with higher roughness than for smoother road surface at same vehicle speeds [9, 10].

The low frequency noise generated by air flowing over a moving car with the open window is chosen as a source of noise (at high velocity behaves as a source of specifically strong tonal annoying noise) and was analysed it within inside the car and its effects on a driver's comfort at different velocities. The interior noise of a passenger car was measured under different conditions; while driving on normal highway and roadways. An octave-band analysis was used to assess the noise level and its impact on the driver's comfort, and a Fast Fourier Transform (FFT) for the detection of tonal low frequency noise, and finally, possibilities for scientifically assessing and evaluating low frequency noise were suggested but not only for the presented source of the sound [11, 12].

The review has shown that almost most studies in the subject of vehicle interior noise comfort (sound quality) are studying of A-weighted noise levels and sound power which are usually utilized to measure the noise, but they are not adequate to characterize the impact sound inside a vehicle. Moreover, the most popular approach to determine sound quality of a product which is to define an annoyance or specific index, which involves both subjective and objective evaluations. The researchers of different automotive acoustics investigations fields can use this index. The objective of this paper is to present an approach to be used to

estimate the vehicle acoustic comfort index depends on the measured and predicted Sound Pressure Level (SPL) at the driver's head position. The predicted SPL was calculated from the vibration of the vehicle floor under the driver's legs region based on the sample acoustic theory.

## 2. Vehicle Interior Noise Prediction

### 2.1. General

There is no simple theory available for prediction of the propagation of sound due to vibration of even a simple structure such as a flat plate. Such a prediction of the propagation can be made by considering the plate as point source. The contributions from that point source can be included in the sound at any given point inside the vehicle body cavity. Then it is possible to determine the sound pressure at that point.

The complex nature of the vibration of a vehicle body structure and its combination with acoustic functions is very difficult to be handled mathematically but for a point on the structure can be measured experimentally. The amount of vibrational energy radiated into the air volume and dissipated in the structure, is controlled by the dynamic characteristics of the vehicle structure panels particularly at resonance.

### 2.2. Mechanism of Noise Generation in a Three-Dimensional Enclosure

When the sound waves are produced in a region completely enclosed by walls, rigid or otherwise, all wave motions, and acoustic-energy content of the cavity are determined by the nature of its walls. Let the enclosure occupies a volume  $V$ , and be surrounded by a wall surface  $S$ , of which the portion  $S_f$  is flexible, while the remainder  $S_r$  is rigid. If the fluid within the enclosure cavity is at rest prior to motion of the walls, the fluid pressure  $P$ , satisfies the familiar wave equations (1 and 2), and associated boundary conditions are:

$$\nabla^2 P(x, y, z) - (1/C^2) \partial^2 P(x, y, z) / \partial t^2 = 0 \quad (1)$$

$$\partial P(x, y, z) / \partial n = -\theta (\partial u(x, y, z) / \partial t) \quad \text{on } S_r,$$

$$\partial P(x, y, z) / \partial n = 0 \quad \text{on } S_f \quad (2)$$

Where:

$\nabla$  Laplacian operator

$C$  Velocity of sound in the relevant medium

$\theta$  Density of  $\partial P(x, y, z) / \partial n = -\theta (\partial u(x, y, z) / \partial t)$

$x, y, z$  Three mutually perpendicular coordinates

In steady state condition, the fluid pressure is defined by  $P = p(x, y, z) e^{j\omega t}$  and equations (1), (2) converted to the following equations (3) and (4):

$$\nabla^2 p(x, y, z) + k^2 p(x, y, z) = 0 \quad (3)$$

$$\partial P(x, y, z) / \partial n = -\theta (\partial u(x, y, z) / \partial t) \quad \text{on } S_r;$$

$$\frac{\partial P(x, y, z)}{\partial n} = 0 \quad \text{on } S_f \quad (4)$$

Where:

- P(x, y, z) Pressure field and a function of space
- U(x, y, z) Velocity of the enclosure wall and a function of space
- N Referred to the normal direction
- K Acoustic wave-number = w/C

In this manner, the time parameter is eliminated, and the computation is reduced to a field problem in the space dimensions only.

### 2.3. Sound Pressure Field Within an Enclose Enclosure [13:15]

Any enclosure cavity has its own natural frequencies. The enclosure such as an automotive body has no exception, and there will be some points fore and aft, other points laterally and vertically at which incident noise will be reinforced and amplified. This is called the standing wave effect of cavity resonance. If the enclosure is considered as a regularly shape (i.e. rectangular) as shown in Figure 1. then the acoustic field enclosed by its smooth parallel walls is established and the standing wave frequencies can be obtained from equation (3) [13].

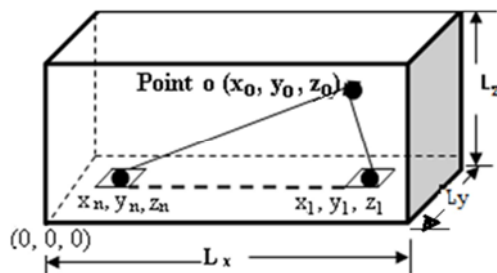


Figure 1. The geometric shape of rectangular enclosure.

The mode shape for each of these frequencies could be obtained from equations (1) and (2), considering the enclosure consisting of one given small element produces a volume velocity within the enclosure cavity. Such that its size is minor compared with the wavelength, the pressure field and the velocity field due to the element are uniform, and the pressure field for the element within the cavity volume V, obeys equation (2). In that way, the following relation is obtained as described by equation (5).

$$\nabla^2 p(x, y, z) + k^2 p(x, y, z) = -(\theta S \omega / V) u(x, y, z) \quad (5)$$

Where:

- u(x, y, z) Average velocity at definite point source placed on definite element
- S An area of that element
- ω Circular angular frequency
- k Wave number = ω/C

The steady-state sound pressure at any point (o) within the enclosure with a point source located at point (x, y, z) on the enclosure walls is a sum of terms of the form equation (6);

$$p(x_o, y_o, z_o) = \sum_m P_m(x_o, y_o, z_o) \quad (6)$$

Each P<sub>m</sub> term is the sound pressure due to point source at (x, y, z) for a normal mode of vibration (standing wave frequencies). This sound pressure has the form equation (7);

$$p_m = P_o e^{-J(k_x x + k_y y + k_z z).r(x, y, z)} \quad (7)$$

Where:

- k<sub>x</sub>, k<sub>y</sub>, k<sub>z</sub> Wave-numbers in three mutually perpendicular directions
- P<sub>o</sub> Pressure amplitude

Each normal mode of vibration has its own normal frequency (natural frequency) ω<sub>m</sub>, obtained from equation (8) and a damping constant α<sub>m</sub>, calculated from ω<sub>m</sub> with the absorption coefficient α<sub>o</sub>, both having the units of radians/sec. The sound pressure associated with one of the terms m at a point o (x<sub>o</sub>, y<sub>o</sub>, z<sub>o</sub>) within the enclosure is as equation (9);

$$\omega_m = f(\text{Hz}) = \frac{C}{2} \left[ \left( \frac{n_x}{L_x} \right)^2 + \left( \frac{n_y}{L_y} \right)^2 + \left( \frac{n_z}{L_z} \right)^2 \right]^{1/2} \quad (8)$$

Where:

- L<sub>x</sub>, L<sub>y</sub>, L<sub>z</sub> Enclosure dimensions in three mutually perpendicular directions
- n<sub>x</sub>, n<sub>y</sub>, n<sub>z</sub> Number of nodes in three mutually perpendicular directions, and are integer values (0, 1, 2 ... etc.)
- C Velocity of sound in the relevant medium (air), 344 m/s
- f(Hz) Enclosure cavity has its own natural frequencies

$$p(x_o, y_o, z_o) = \sum_m \frac{\theta S \omega u(x, y, z) Q_m(x, y, z)}{v(k_m^2 - k^2)} \quad (9)$$

Where:

- k<sub>m</sub> Wave number of a normal mode = (ω<sub>m</sub> + J α<sub>m</sub>) / C
- Q<sub>m</sub>(x, y, z) Sound pressure distribution for each normal mode m, of a point source =  $\cos\left(\frac{\Pi n_x x}{L_x}\right) \cos\left(\frac{\Pi n_y y}{L_y}\right) \cos\left(\frac{\Pi n_z z}{L_z}\right)$

In the case of forced vibration, the damping term α<sub>m</sub>, is added to wave number of the normal mode to avoid the divergence of the solution. Then equation (9) can be rewritten as equation (10):

$$p(x_o, y_o, z_o) = \sum_m \frac{\theta S \omega C^2 u(x, y, z) Q_m(x, y, z)}{v \left[ (\omega_m + J \alpha_m)^2 - \omega^2 \right]^2} \quad (10)$$

If the enclosure walls contain several such point sources (see Figure 1), then the contributions to the sound pressure made by the individual sources at points (x<sub>1</sub>, y<sub>1</sub>, z<sub>1</sub>), (x<sub>2</sub>, y<sub>2</sub>,

$z_2$ ), ..... ,  $(x_n, y_n, z_n)$  from the point  $o(x_o, y_o, z_o)$  within the enclosure are given by equation (11). Because of the surface velocity in equation (11) is a complex quantity, this relation will be applied the even if the sources of all over the enclosure walls vibrate with various phase angles between one another.

$$p(x_o, y_o, z_o) = (\theta C^2 \cdot \omega / V) \sum \sum_{nm} \frac{S_n u_n(x, y, z) Q_{nm}(x, y, z)}{\left[ (\omega_m + J\alpha_m)^2 - \omega^2 \right]} \quad (11)$$

Where:

- $u_n(x, y, z)$  Average velocity of a point source placed on a definite element
- $S_n$  Area of that element
- $\theta$  Density of the relevant medium
- $C$  Velocity of sound in the relevant medium
- $\omega_m$  Angular normal frequency of the cavity
- $\alpha_m$  Damping constant =  $-\omega_m \cdot \ln(1 - \alpha_o)$
- $\omega$  Circular frequency

### 3. Human Perception of Sound

The strength of sound measured by a sound level meter in its simplest form, gives SPL in dB. SPL does not consider the nonlinearity of our perception with respect of frequency, as reflected in the concept of loudness. To better reflect the human perception of sound, sound level meters contain filters, so-called weighted filters that amplify the microphone signal with different amounts at different frequencies. One of these filters is A-weighted which is the most common below 1000 Hz. The amplification is negative implying that these frequencies are damped to compensate for the lower sensitivity of mankind to low frequency sound. A-weighting is taken from 40 phone curves. Originally, the thought was that A-weighting would be used at low SPL, thereby adjusting the measurement results to our perception of sound as it varies in both frequency and strength. In this paper, however, A-weighting sound pressure level ( $SPL_A$ ) is most often used. A  $SPL_A$  that is measured or predicted with A-weighting filter, is called sound level ( $L_A$ ). Assume that the measured  $L_A$  with an A-weighting filter is 75 dB. That is written as  $L_A = 75 \text{ dB (A)}$ . Current standards recommend that if the input motion at low frequency, Vehicle Interior Noise Comfort Index (VINCI) value is determined using dB (A)

measured and  $\text{dB (A)}_{\text{predicted}}$  at the driver's head position, as equation (12):

$$VINCI = \frac{SPL_A, \text{dB (A)}_{\text{measured}}}{SPL_A, \text{dB (A)}_{\text{predicted}}} \quad (12)$$

## 4. Experimental Data Measurements

### 4.1. General

In this measurement, response channel was the vehicle floor vibration and involvement of only two references, i.e. tire-road and engine-transmission vibration was investigated. The accelerometer mounting is one of the most critical factors in achieving accurate results. Poor attachment reduces the mounted resonance frequency and severely limits the useful frequency range of the accelerometer.

Epoxy hard glue only slightly reduces the resonance frequency and was a good choice for measurement in moving condition. Triboelectric noise was prevented by using low noise cables which were fixed to the structure by adhesive tape. Rechargeable power supply labshop and printer are the most important attachment to the analyzer as shown in schematically Figure 2. Bruel and Kjaer instrumentation series (namely, portable and multi-channel analyzer PULSE type 3560D, PULSE Labshop.

### 4.2. Vehicle Floor Vibration

The vibration measurements were made in the road surface textures and the vibration signals were acquired with integration period of 1.0 second. The vibration acceleration signals in terms of time domain on the floor were measured in vertical direction and considered as a reference vibration signal by using Bruel & Kjaer accelerometer Type 4514B-001 mounted upon the vehicle floor as shown in Figure 3. The vibration amplitudes recorded from floor during coast down with unloaded engine (neutral gear) were conducted for possible artifacts and any unclear signals detected are removed. The vibration acceleration measured was truncated to show the frequency range of interest which is up to 400 Hz. The measurements were carried out for vehicle speed from 20 km/hr to 80 km/hr.

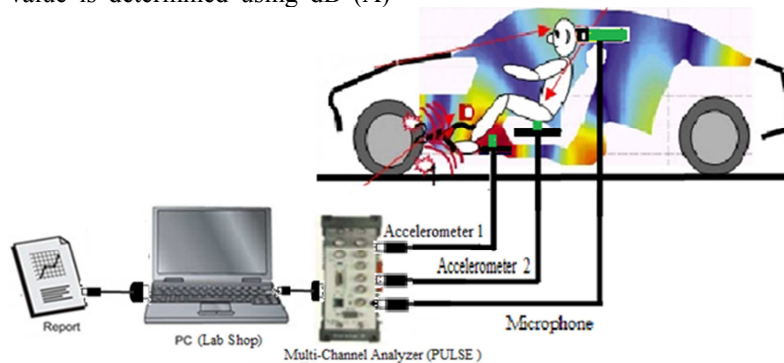


Figure 2. Schematic diagram of the experiment assembly.

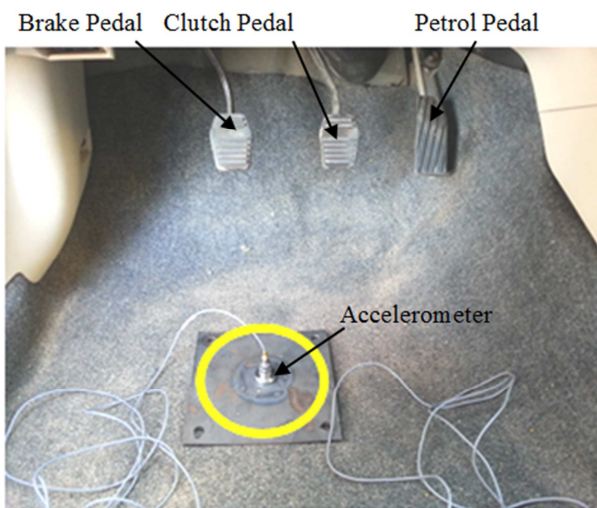


Figure 3. Vehicle floor accelerometer position.

### 4.3. Vehicle Interior Noise

Practical measurements of interior road noise were conducted during coast down with unloaded engine (neutral gear). One microphone was positioned at the driver's head position, horizontally, pointing with their maximum sensitivity direction as shown in Figure 4. The vibration amplitudes recorded from floor during coast down with unloaded engine (neutral gear) were conducted for possible artifacts and any unclear signals detected are removed. The noise in terms of sound pressure level measured was truncated to show the frequency range of interest which is up to 400 Hz and for vehicle speed from 20 km/hr to 80 km/hr. A-weighting of dB sound pressures level reveals tonal aspects (speed dependent) related to tire rotation frequency as well as constant resonance characteristics.

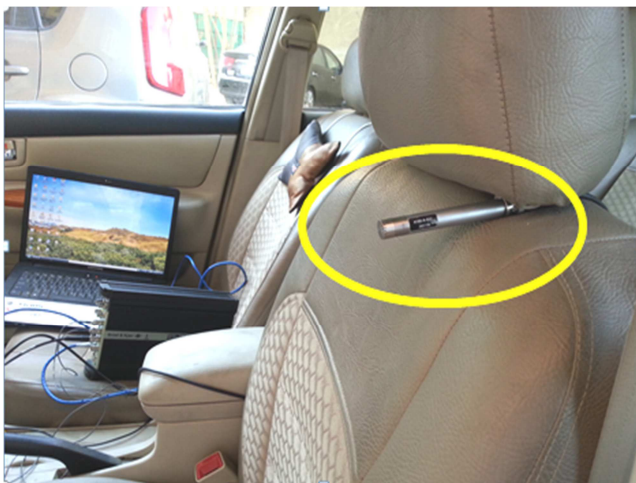


Figure 4. Microphone/condenser position.

### 4.4. Experimental Procedure

The test vehicle was a mid-size executive vehicle, where its chassis and body dimensions' specifications are presented in Table 1. The vehicle handles well through tight corners and has a good high-speed cruiser. The vibration signals were measured while the vehicle was in coast down conditions over three flat road surfaces (asphalt, sand and Gravel) as presented in Table 2 with the road surfaces characteristics. The Asphalt had a flat, smooth surface and occasional unevenness, which resulted in minimum disturbances. The tire technical specifications are tabulated in Table 3, while Figure 5. shows the type of tires used in this work.

Table 1. Vehicle Body Dimensions' Specifications.

No.	Parameter	Specification	Value
1	Vehicle class	Midsized sedan	--
2	Layout	Front engine	--
		Front wheel drive	--
3	Dimensions	Overall length (mm)	4533
		Overall width (mm)	1705
		Vehicle height (mm)	1490
4	Cavity dimensions	Length, Lx (mm)	2600
		Width, Ly (mm)	1200
		Height, Lz (mm)	1200
5	Wheel base (mm)		2600
6	Wheel track	Front (mm)	1480
		Rear (mm)	1460
7	Curb weight (kg)		1200
8	Total weight (kg)		1575
9	Tire		195/60 R15-91H

Practical measurements of vehicle interior vibration and noise were conducted during coast down with unloaded engine (neutral gear).

One microphone was positioned at the driver's head position. Microphone was placed almost horizontally, pointing with their maximum sensitivity direction. The A-weighting of the dB sound pressures level reveals tonal aspects (speed dependent) related to tire rotation frequency as well as constant resonance characteristics. Noise and vibration originate during coast down were conducted as a good representative source of strong low frequency noise. During the measurements, the vehicle was driven on the road surfaces with minimal traffic, i.e. the aim was to minimize the influence of other sources of vibration and noise from passing vehicles. The measurements were done at various vehicle speeds during coast down drive ranging from 20 km/hr to 80 km/hr. The noise was measured at the driver's head position, i.e. the microphone was positioned close to the head, to analyse the effect of the noise on the driver while driving the vehicle.

**Table 2.** Description of Road Surface Textures.

Road Type	Road surface appearance	Road surface characteristics	Road surface texture
Smooth Asphalt	Smooth asphalt, no wear or weathering, small stones	Low overall level, higher frequency greater proportion of noise, no "roar"	
Sand	Sandy soils and size distribution of fine sand, and greater porosity.	Are often dry, nutrient deficient and fast-draining, water retention and resistance to penetration, they exhibit lower permeability.	
Gravel	Pattern not complete random, polished stones, moderately dense aggregate	high max stone size, high overall level.	



**Figure 5.** Tire types: (a) 195/60- R15 (b) 185/65-R15 and (c) 195/65- R15.

**Table 3.** Tires Technical Specification.

Technical Details	Bridgestone Data		
	195/60	185/65	195/65
Description	R15 88H	R15 88H	R15 91H
Model	AR20 (Original)	B250	ER-300
Weight, Kg	8	8	8
Tyre	Tubeless	Tubeless	Tubeless
Circumference, mm	1932	1952.5	1993.34
Radius, mm	307.5	310.75	317.25
Sidewall Height, mm	117	120.25	126.75
Overall Diameter, mm	615	621.5	634.5
Section Width, mm	195	185	195
Aspect Ratio, %	60	65	65
Construction	R	R	R
Rim Diameter, mm	381	381	381
Load Index Rating	88	88	91
Load Carrying Capacity, kg	560	560	615
Max. Speed km/hr	210	210	210

## 5. Results and Discussion

### 5.1. Predicted SPL

The vehicle body structure is in trimmed conditions, where the prediction of interior SPL is in terms of cavity normal modes which calculated based on equation (5) and the cavity dimensions (mm) presented in Table 1, where the velocity of sound in the relevant medium C is 344 m/s. The vehicle body cavity is considered as a regularly shape (i.e. rectangular) then the acoustic field enclosed by its smooth parallel walls is established and the standing wave frequencies can be obtained. The results of the frequency range used in this work (i.e., 200 Hz) and are tabulated in Table 4.

**Table 4.** Vehicle Cavity Normal Modes.

Nodes			Cavity dimensions			Resonant Frequency	
$n_x$	$n_y$	$n_z$	$L_x$	$L_y$	$L_z$	f, Hz	$\omega$ , rad/s
1	0	0	2.6	1.2	1.2	66.15385	415.4462
0	1	0	2.6	1.2	1.2	143.3333	900.1333
0	0	1	2.6	1.2	1.2	143.3333	900.1333
1	1	0	2.6	1.2	1.2	157.8632	991.3806
1	0	1	2.6	1.2	1.2	157.8632	991.3806
2	0	0	2.6	1.2	1.2	132.3077	830.8923
2	1	0	2.6	1.2	1.2	195.0635	1224.999
2	0	1	2.6	1.2	1.2	195.0635	1224.999
3	0	0	2.6	1.2	1.2	198.4615	1246.338
1	0	0	2.6	1.2	1.2	66.15385	415.4462

As stated previously that the vibration of vehicle body

structure or part of it cannot be expressed as a simple mathematical function. This means that the vibration velocity  $u_n$  presented in equation (11) needs to be measured, where the volume of the cavity  $V$  is  $3.744 \text{ m}^3$  and the density of the relevant medium ( $\theta$ ) is  $1.22 \text{ kg/m}^3$ . The purpose of applying the previous approach for small area ( $S$ ) of  $0.0625 \text{ m}^2$  within the vehicle floor, where a vibration velocity can be determined. Therefore, the prediction of SPL resulting from the vibration of the vehicle floor element will be an approximate value. The vibration velocity was measured in the centre of the vehicle floor element.

## 5.2. Vehicle Interior Noise Comfort Index

### 5.2.1. Influence of Vehicle Payload

Figures 6. and 7. show samples for the results of the frequency domain for the vehicle floor vibration velocity and time history of SPL measured at vehicle speed of 80 km/hr, Figure 8. shows a comparison between the measured SPL on the experimental procedure presented herein at item 4.4 and predicted SPL estimated based on equation (11) in terms of frequency domain. The same trend can be observed in the two curves with various levels. Figure 9. illustrates VINCI value calculated from equation (12) with respect to vehicle speed of 20, 40, 60 and 80 km/hr respectively at different vehicle payload of 150 kg, 225 kg and 300 kg. It can be observed that VINCI value is limited at low speed of 20 km/hr, while at the other vehicle speeds considered, VINCI value at vehicle payload of 150 kg indicates a best level.

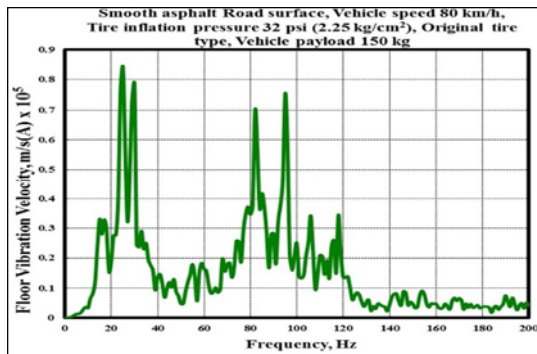


Figure 6. Frequency domain of the vehicle floor vibration velocity.

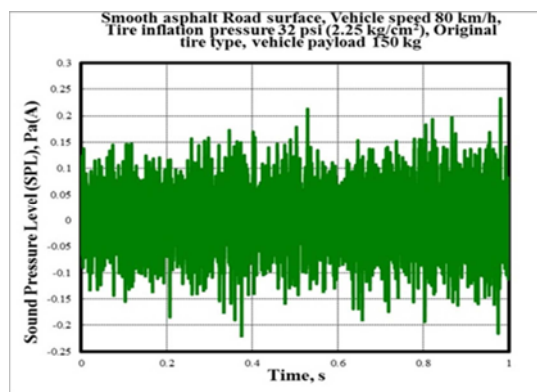


Figure 7. Time history of the measured sound pressure level at driver's Head.

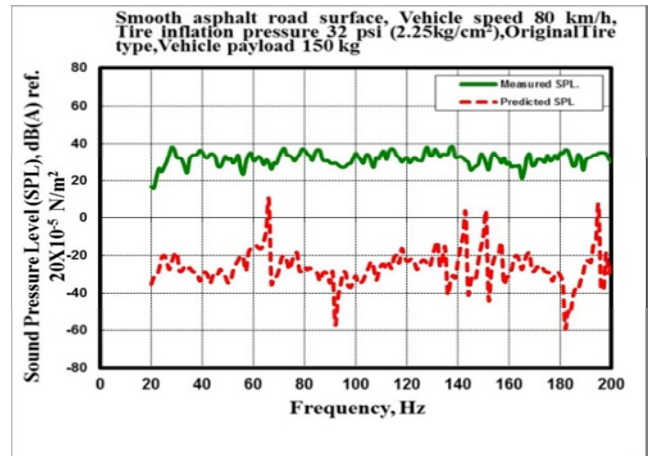


Figure 8. Sound pressure level at driver's head position at 80 km/h.

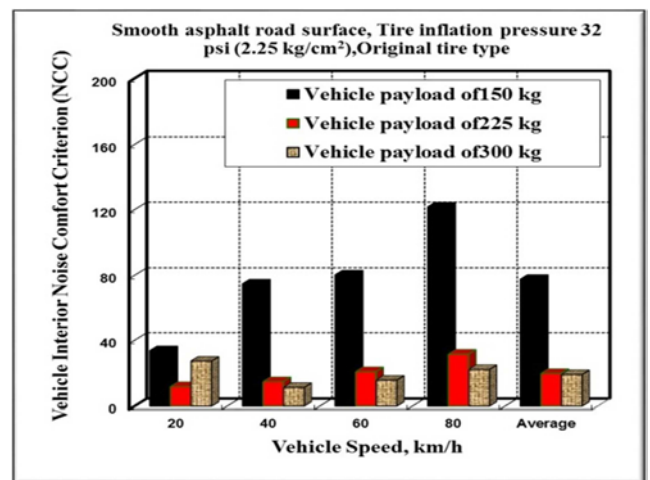


Figure 9. Calculated VINCI.

### 5.2.2. Influence of Road Surface Texture

Figures 10. and 11. show samples for the results of the frequency domain for the vehicle floor vibration velocity and time history of SPL measured at vehicle speed of 60 km/hr. Figure 12. shows a comparison between measured SPL on the experimental procedure presented herein at item 4.4 and predicted SPL estimated based on equation (11) in terms of frequency domain. The same trend can be observed in the two curves with diverse levels. Figure 13. illustrates VINCI value calculated from equation (12) with respect to vehicle speed of 20, 40, 60 and 80 km/hr respectively at different road surface texture as tabulated and seen in Table 2. It can be observed that VINCI value at gravel road surface texture has the highest value at vehicle speed of 20 km/hr for the vehicle speeds considered then increased till speed of 80 km/hr, while for sand road surface texture has lowest values with the highest value at vehicle speed of 60 km/hr. The best VINCI value is observed for the use of smooth asphalt all over the entire vehicle speeds considered. This is clearly seen in the average values. In addition, VINCI value has a medium to high correlation with the vehicle speed. Whereas, sand road surface texture has no meaningful relationship with VINCI because the correlation is very low except for gravel

and smooth asphalt road surface textures.

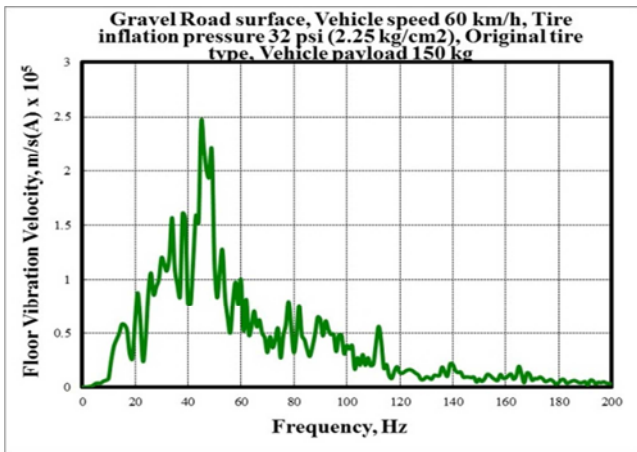


Figure 10. Frequency domain of the vehicle floor vibration velocity.

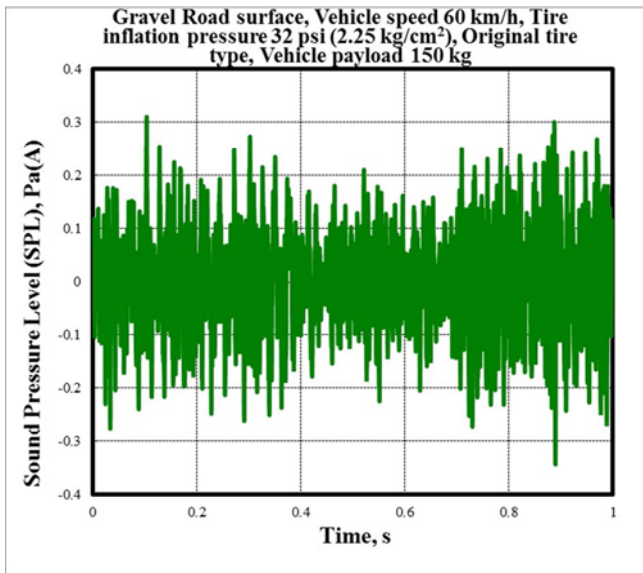


Figure 11. Time history of the measured sound pressure level at driver's head.

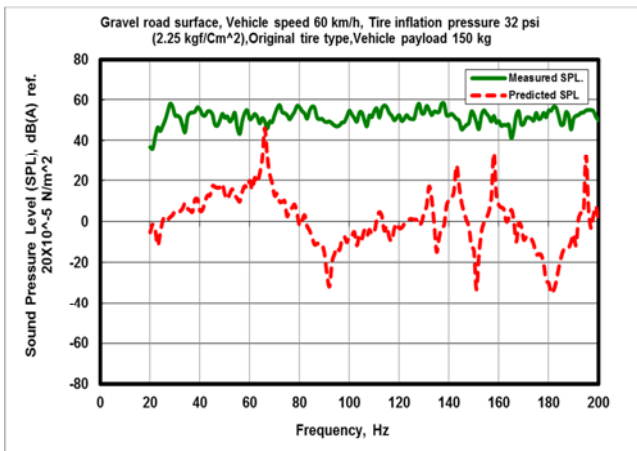


Figure 12. Sound pressure level at driver's head position at 60 km/h.

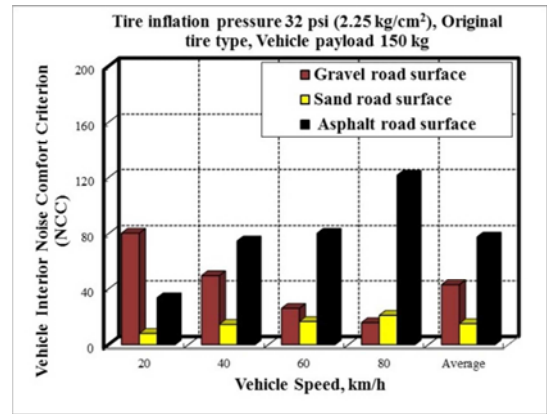


Figure 13. Calculated VINCI.

### 5.2.3. Influence of Vehicle Tire Inflation Pressure

Figures 14. and 15. show samples for the results of the frequency domain for the vehicle floor vibration velocity and time history of SPL measured at vehicle speed of 40 km/hr. Figure 16. shows a comparison between the measured SPL on the experimental procedure presented herein at item 4.4 and predicted SPL estimated based on equation (11) in terms of frequency domain. The same trend can be observed in the two curves with distinct levels. Figure 17. illustrates VINCI value calculated from equation (12) with respect to vehicle speed of 20, 40, 60 and 80 km/hr respectively at different vehicle tire inflation pressure of 28 psi ( $1.97 \cdot 10^4$  kg/m<sup>2</sup>), 32 psi ( $2.25 \cdot 10^4$  kg/m<sup>2</sup>) and 36 psi ( $2.54 \cdot 10^4$  kg/m<sup>2</sup>). It can be observed that VINCI value at vehicle tire inflation pressure of 32 psi ( $2.25 \cdot 10^4$  kg/m<sup>2</sup>) has the highest value at all the vehicle speeds considered, followed by 36 psi ( $2.54 \cdot 10^4$  kg/m<sup>2</sup>) with the least for 28 psi ( $1.97 \cdot 10^4$  kg/m<sup>2</sup>). This is clearly seen in the average values. In addition, VINCI value as a medium to high correlation with the vehicle speed. Whereas, the vehicle tire inflation pressure of 28 psi ( $1.97 \cdot 10^4$  kg/m<sup>2</sup>) has no meaningful relationship with VINCI because the correlation is very low except for both 32 psi ( $2.25 \cdot 10^4$  kg/m<sup>2</sup>) and 36 psi ( $2.54 \cdot 10^4$  kg/m<sup>2</sup>).

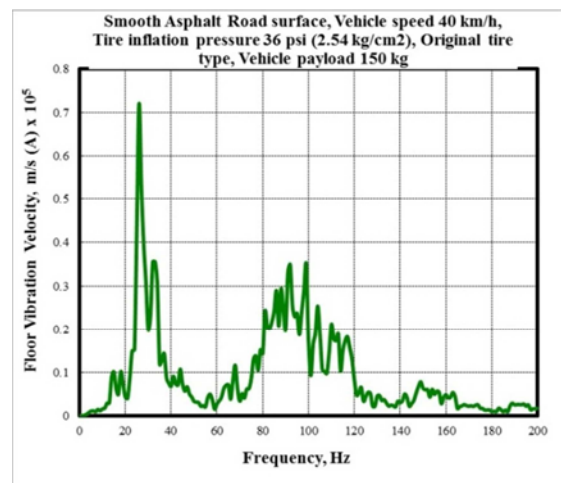


Figure 14. Frequency domain of the vehicle floor vibration velocity.

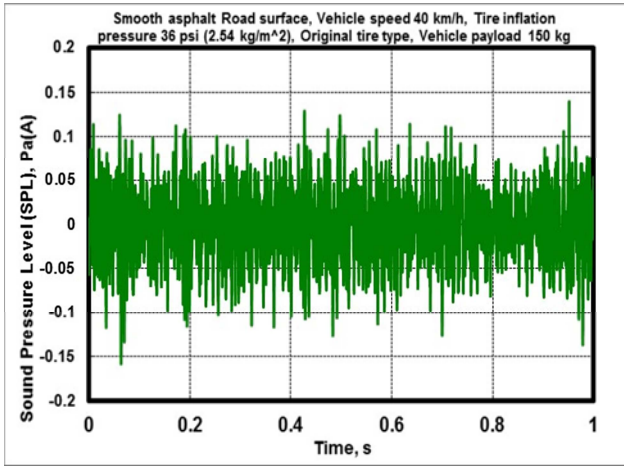


Figure 15. Time history of the measured sound pressure level at driver's head.

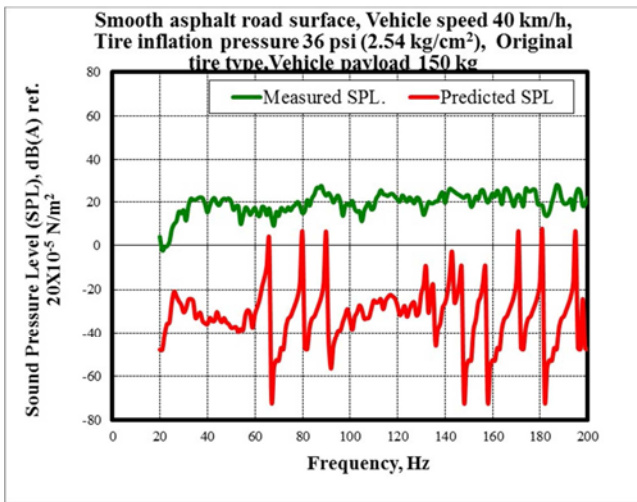


Figure 16. Sound pressure level at driver's head position at 40 km/h.

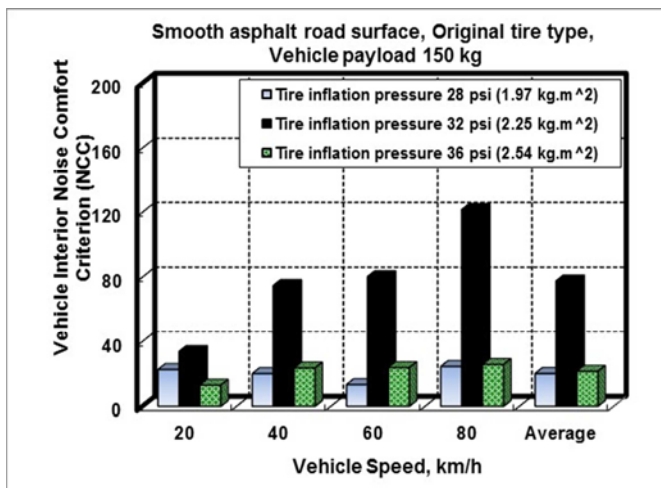


Figure 17. Calculated VINCI.

### 5.2.4. Effect of Vehicle Tire Types

Figures 18. and 19. show samples for the results of the frequency domain for the vehicle floor vibration velocity and time history of SPL measured at vehicle speed of 20 km/hr respectively, while Figure 20. shows a comparison between the

measured SPL on the experimental procedure presented herein at item 4.4 and predicted SPL estimated based on equation (11) in terms of frequency domain. The same trend can be observed in the two curves with distinct levels. Figure 21. illustrates VINCI value calculated from equation (12) with respect to vehicle speed of 20, 40, 60 and 80 km/hr at different tire types of 185/60-R15-88H (B250), 195/60-R15-88H AR20 (Original) and 195-65- R15 -91H (ER-300). VINCI due to tire-road interaction studied in this paper can be used related to the types of the vehicle tire, without the need to perform time-consuming jury tests. For instance, VINCI inside the vehicle cavity has high correlation with ehicle speed. A straight forward relationship exists which means that whenever the vehicle speed increases, VINCI increases. In addition, the original tire type (195/60-R15-88H AR20) has the highest VINCI value. Whereas, the other two types have nearly the same VINCI with no meaningful relationship because the correlation is very low. VINCI due to tire-road interaction studied in this paper can be used related to the types of the vehicle tire, without any need to perform time-consuming jury tests. For instance, VINCI inside the vehicle cavity has high correlation with vehicle speed.

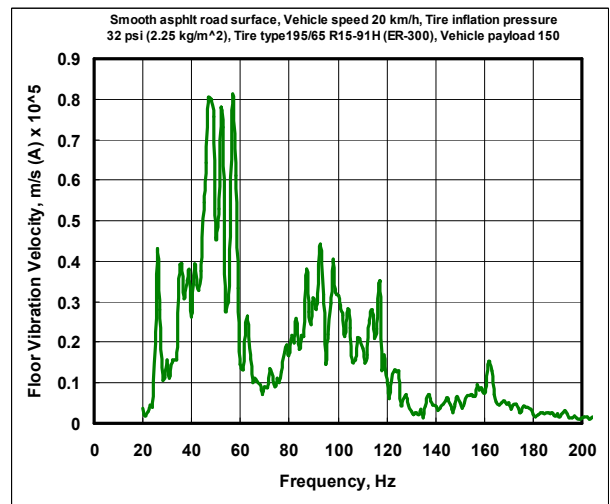


Figure 18. Frequency domain of the vehicle floor vibration velocity.

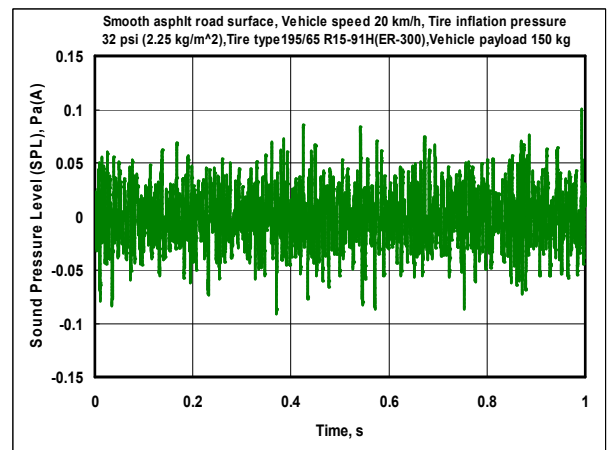


Figure 19. Time history of the measured sound pressure level at driver's head.

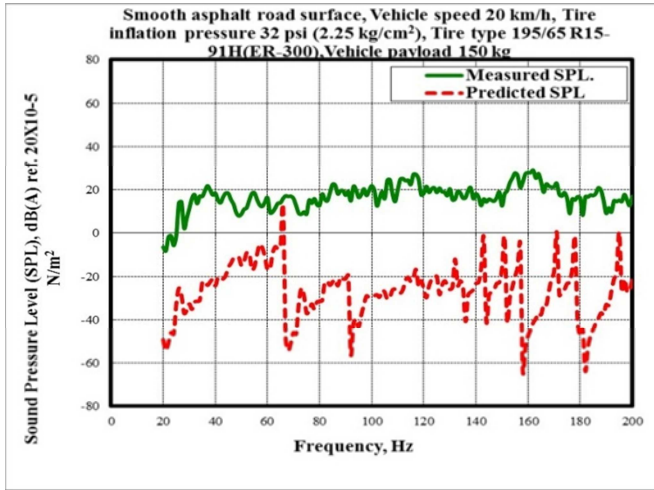


Figure 20. Sound pressure level at driver's head position at 20 km/h.

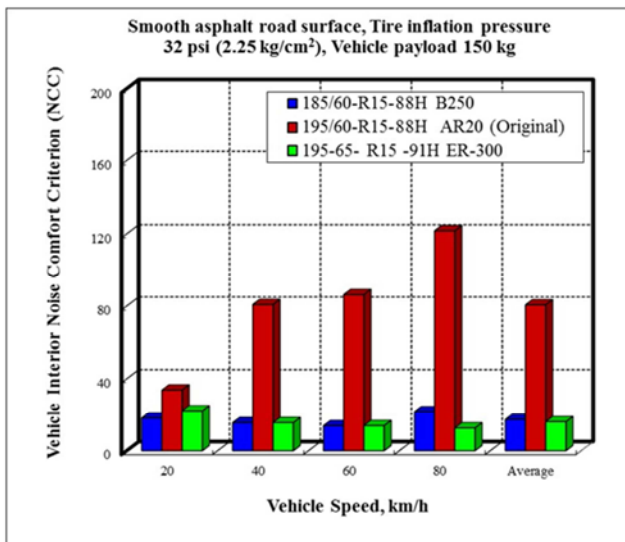


Figure 21. Calculated VINCI.

## 6. Conclusion

1. The amount of noise level which produced by the interactions between tires and road surface it can be concluded that the increase of vehicle speed can influence the noise level by increasing the value of VINCI; in other words, with the increase of vehicle speeds it may cause more noise due to the vibration from interaction between tire and road surface.
2. An average VINCI value due to tire-road interaction studied in this paper can be used according to the type of road surface, vehicle payload, type of tire and tire inflation pressure without any need to perform time-consuming jury tests. For instance, an average VINCI value has high correlation with inverse relationship which means that whenever vehicle payload increases, the vehicle acoustical comfort decreases.
3. The best VINCI value is observed for the use of smooth asphalt all over the entire vehicle speeds considered. This is clearly seen in the average values. In addition,

VINCI value has a medium to high correlation with the vehicle speed. Whereas, sand road surface texture has no meaningful relationship with VINCI value because the correlation is very low except for gravel and smooth asphalt road surface textures.

4. A novel approach was proposed for evaluating annoyance of vehicle interior noises. The noise signals under different working conditions of a sample vehicle were measured and saved. VINCI value, such as measured sound pressure level measured and predicted from the vehicle floor vibration, were mathematically derived and calculated. The approach can be directly used to estimate and compare sound quality of vehicles, and its applications will be promising research topics in the future.
5. The amount of noise caused by the tire interaction with the road surface was found. To obtain some amount of noise, an experiment was carried out and performed the data analysis from the first to the last stage, based on the procedures explained herein. As seen in the data analysis, the characteristics of the road surface texture serve as a major contributor to the existed noise in the vehicle cavity. Since different road surfaces affect the noise level that is generated, it was very important to us to consider and take note of the specifications and patterns of the tires surfaces.

## References

- [1] Siano, D, Prati, M. V., Costagiola, M. A. and Panza, M. A., (2015), "Evaluation of Noise Level Inside Cab of a Bi-Fuel Passenger Vehicle" WSEAS Transactions on Applied and Theoretical Mechanics, Vol. 10, 220-225.
- [2] Mohammadi, N., (2015), "Analytical and Experimental Evaluation of Cabin Noise Sources of MB 1924 Truck and its Acoustic Treatment" International Journal of Engineering & Technology Sciences Vol. 3, Issue 2, 178-194.
- [3] Junoh, A. K., Nopiah Z. M., Abdul, A. H., Nor M. J. M., Ihsan, A. K. A. M. & Fouladi, M. H., (2012), "A Study to Predict the effects of Tires Vibration to Sound Quality in Passenger Car Cabin" International Journal of Engineering (IJE), Vol. (6): Issue (1), 53-69.
- [4] Junoh, A. K, Nopiah, Z. M., Muhamad, W. Z. W., Nor, M. J. M. and Fouladi, M. H., (2012), "An Optimization Model of Noise and Vibration in Passenger Car Cabin" Advanced Materials Research Vols 383-390, 6704-6709.
- [5] Sottek, R and Philippen, B, (2010), "Separation of Airborne and Structure-Borne Tire-Road Noise Based on Vehicle Interior Noise Measurements" Society of Automotive Engineers (SAE) 2010, Technical Paper, Paper No. 2010-01-1430.
- [6] Pang, J., Zhang, J., Zhang, J., Chunmin Xu, C and Jia, W., (2014), "A Simplified Model for Vehicle Body Panel Vibration and Sound Radiation and Interior Booming Control" The 21st International Congress on Sound and Vibration, Beijing/China, 13-17 July.
- [7] Liao, X. Zheng, S, Peng, B. and Lian, X., (2014), "A Playback System for Sound Quality Evaluation of Interior Noise" The 21st International Congress on Sound and Vibration, Beijing/China, 13-17 July.

- [8] Zhang, L., Pan, J. and Qiu, X., (2014), "Effects of a passive Enclosure on an Active Noise Control System in Free Field " The 21st International Congress on Sound and Vibration, Beijing/China, 13-17 July.
- [9] Abouel-Seoud, S. A., (2015), "Influence of Road Roughness Parameters on Low Frequency Interior Noise in Off-road and Mid-Size Passenger Vehicles" International Journal of Vehicle Structures and Systems, 7 (2), 71-76.
- [10] Ziaran, S., (2013), "Low Frequency Noise and Its Assessment and Evaluation", Archives of Acoustics, Vol. 38, No. 2, 265–270.
- [11] Kindt, P., De Coninck, F., Sas, P. and Desmet, W., (2006), "Test Setup for Tire/Road Noise Caused by Road Impact Excitations: First Outlines", Proceedings of ISMA.
- [12] Khalil, M. I., Mansy, M. N., Saad, A. A. and Abouel-seoud, S. A., (2012), "Vehicle-road interaction for interior noise measurement and evaluation", Int. J. Vehicle Noise and Vibration, Vol. 8, No. 4.
- [13] Beranek, L. L. and Vér, I. L., (1992), "Noise and vibration control engineering" Principles. Applications, John Wiley & Sons, Inc, Chapter 6.
- [14] Beranek, L. L., (1971), "Noise and vibration control "book, Mac Grew-Hill.
- [15] Pan, J. and Bies, D. A., (1990), "The Effect of Fluid-structural Coupling on Sound Waves in an Enclosure – Theoretical Part" Journal of Acoustical Society of America, 87 (2), 691–707.